# Buffer-Constrained Throughput Analysis of a Wireless-Powered Communication Network

Zhidu Li, *Student Member, IEEE,* Yuming Jiang, *Senior Member, IEEE,*
Yuehong Gao, Lin Sang, and Dacheng Yang

***Abstract*—In this paper, the buffer-constrained throughput performance of a multi-user wireless-powered communication system is investigated with a practical non-linear energy harvesting model. The investigation focuses on the backlog performance of sending data in the downlink (DL) from the access point (AP) node to each user equipment (UE) node and that in the uplink (UL) from the UE node to the AP node, based on which, the throughput performance on both directions when buffer constraints are enforced is also studied. To this aim, the buffer overflow probability is derived for each communication node with given data buffer capacity. Based on the buffer constraint, the buffer-constrained throughput is then ascertained. In addition, to ensure the buffer and throughput performance, the DL transmission power allocation policy and the required energy storage capacity are investigated. Moreover, a non-convex max-min problem is formulated to maximize the minimum buffer-constrained throughput guaranteed by each UE simultaneously. A dichotomy-based time allocation algorithm combined with one-dimensional search is proposed to solve this problem. The obtained results explicitly reveal the maximum traffic throughput sustained by each node is dominated by energy harvesting model, buffer constraint, channel path loss, time allocation scheme and the number of UEs. The analysis and results shed new light on the performance of wireless-powered communication systems.**

***Keywords*—Wireless-powered communication system, buffer performance, buffer-constrained throughput, resource allocation.**

## I. Introduction

With the advance of wireless charging technology [1, 2], wireless powered communication (WPC) has recently attracted a significant amount of attentions in both academia and industry [3–6]. In a WPC system, a number of nodes, e.g. user equipments (UEs), harvest energy and may simultaneously also receive data from the ambient radio frequency (RF) signals that may be purposely radiated by another node, e.g. an access point (AP), in its downlink (DL) to the UE nodes, and then the UE nodes may use the harvested energy to transmit data in the uplink (UL) to the AP node, as shown in Fig. 1. Compared to the natural renewable energy sources such as solar and wind, RF signal is more controllable and relatively stable [7]. Additionally, due to long lifetime, WPC devices are more accessibility and deployability than the conventional battery-powered devices in extreme environments, such as the hazardous area and the human body, where replacing batteries is difficult or even impossible [1]. As a result, WPC has a great potential for use in a wide range of applications particularly in wireless sensor networks (WSNs) and Internet of Things/Everything (IoT/IoE) [3, 8].

Typically, a fundamental issue of the WPC system is to decide how much time should be allocated to the AP for wireless energy and information transfer and to each communication node for data transmission [7–20]. To answer this question, one has to investigate how much data needs to be sent by the AP node in the DL and how much by the UE nodes in the UL, or equivalently what data throughput or capacity the system is intended to achieve for the AP and each UE respectively. In addition to channel capacity, data buffer overflow control is sometimes also required by some WPC devices. For instance, buffer requirement is a crucial consideration for a large-scale wireless sensor network where resource of a single node is limited since the size and production cost of devices are usually required as small as possible [21]. Moreover, due to hardware limitation and imperfect energy transfer, the amount of harvested energy in a WPC system may be highly limited compared with the conventional systems powered through circuit [2]. As a consequence, if there is backlog requirement on the data, e.g., the buffer overflow probability, the investigation of a WPC system should also take the backlog into account. These constitute the objective of this paper.

In this paper, we investigate the buffer-constrained throughput performance of a multi-user WPC system with finite data buffer capacity. Specifically, our focus is on the backlog performance of each node including the AP and UEs, and on their maximum throughput performance when buffer constraints are enforced. In our investigation, practical non-linear energy harvesting model, finite energy storage capacity, stochastic traffic and stochastic fading channel are taken into account. To this aim, the buffer overflow probability for stochastic traffic arrivals are derived for each node based on which the buffer-constrained throughput of each node is further derived. Moreover, the system resource allocation policies are studied to guarantee the buffer overflow probability and traffic throughput performance. More specifically, we first derive a DL power allocation policy to satisfy the performance requirements of all the nodes in both DL and UL. The minimum battery capacity is then obtained after ensuring the harvested energy is sufficient. Finally, to deal with the doubly near-far problem in a WPC system [9], an optimal time allocation algorithm was proposed to maximize the minimum buffer-constrained throughput which can be guaranteed by each UE simultaneously.

The contributions of this paper is summarized as follows:

- This paper develops a tractable framework to study the backlog and throughput performance together for both DL and UL data transmissions in a multi-user WPC system with finite buffer capacity. The proposed

framework is universal since the analysis takes practical energy harvesting model, finite energy storage capacity, stochastic traffic and stochastic fading channel into account. Particularly, buffer overflow probability is derived in close-form. The buffer-constrained throughput is not only able to inform each node how much data can be accessed under a given buffer constraint, but also converges to the results in [7] when buffer constraint is loosen infinitely.

- The DL power allocation policy and energy storage capacity configuration are designed to guarantee the buffer-constrained throughput performance from probabilistic point of view while comparing to our early work [20] where the resource allocation policies are only designed to guarantee performance in averages.
- This paper proposes a dichotomy-based time allocation algorithm to deal with the doubly near-far problem where the minimum buffer-constrained throughput guaranteed by each UE simultaneously is maximized. Specifically, we first fix the energy transfer time of each TB and use dichotomy approach to find out the time allocation solution which ensures each UEs experiences identical buffer-constrained throughput. The the optimal time allocation is then ascertained by one-dimensional search.
- The analysis results explicitly reveal the impacts of energy harvesting model and time allocation policy on throughput performance when buffer constraints are enforced. They shed new light on the performance of WPC systems.

### A. Related Work

In the literature, a number of studies on the throughput performance of WPC systems can be found. Usually, these studies only focus on either UL or DL transmission. *On UL transmission*, work [9] was the first time to propose time allocation schemes to maximize throughput in a multi-user WPC system. Based on the proposed harvest-then-transmit protocol, the maximum system throughput and the maximum common throughput which can be guaranteed by all the UEs at the same time were obtained by solving optimization problems. In [10], the focus was on spatial UL throughput maximization of a large-scale WPC network. The optimal tradeoff between the energy transfer and information transfer was found out by using stochastic geometry theory. In [11], an optimization algorithm was proposed to maximize the system UL throughput in a multiuser multi-input-multi-output (MIMO) system through jointly optimizing the energy beamforming, receive beamforming and time slot allocation. In [12], the optimal time allocation scheme was studied to maximize the average throughput in both delay-limited mode and delay-tolerant mode which are differentiated through whether the code length is finite or not. Different from works [9–12] where the energy harvesting efficiency at the UE circuit was assumed to be constant, in [7, 13], the authors employed a practical non-linear energy harvesting model to study throughput performance and revealed the inaccuracy of throughput results while using the conventional linear model. In [8], the impact of DL wireless power transfer on the UL transmission throughput was investigated. A unified framework was then presented to optimize the system throughput under both time split and power split schemes. *On DL transmission*, the studies usually address in the rate-energy (R-E) tradeoff of the simultaneous wireless information and power transfer (SWIPT) technology. In [14], the R-E tradeoffs were studied for single-antenna terminals under four typical SWIPT schemes. In [15] and [16], the R-E tradeoffs were studied for MIMO broadcasting channels under linear and non-linear RF energy harvesting models respectively. In [17], the R-E tradeoff was analyzed in the regime of finite code length with consideration of decoding error probability.

In summary, the throughput performance studied in the existing works [7–17] is equivalent to the channel capacity due to the concealing assumption of saturate traffic. To the best of our knowledge, the state-of-the-art study of WPC systems rarely focus on buffer overflow probability. Only a few works try to investigate the WPC systems from the viewpoint of delay. In [18], a method to control the power-delay tradeoff on demand in a WPC system was proposed to minimize the time-averaged power consumption. In addition, work [19] proposed an adaptive harvest-then-cooperate protocol to minimize the average delay of UE by simulation method. However, the aims of [18, 19] are both with little touch on maximizing the throughput or capacity performance as in [7–17]. In our early work [20], we focused on a point to point WPC scenario. The delay and delay-constrained throughput performance was analyzed for both DL and UL transmission. However, as shown in [20], the delay of most packets are usually smaller than one charging cycle in the WPC systems. Therefore, if the charging cycle is small enough, the delay is no longer the major constraint in a WPC system. At this time, the backlog performance is more worth studying since the buffer overflow phenomenon may be more prominent for a device with small buffer capacity.

The remainder is organized as follows. In Section II, the system model is presented. In Section III, general analysis of the WPC system is conducted. In Section IV, the resource allocation policies are studied. In Section V, analytical results are presented, compared and discussed. Finally, we conclude the paper in Section VI.

## II. System Model

### A. Notation

Throughout this paper, the following notations are adopted. A variable with subscript $k$ means it is used for the AP ($k = 0$) or the $k$th UE ($k \geq 1$) which is denoted by $U_k$. Variables $s$ and $t$ are always used to identify the transmission blocks. The cumulative amount of stochastic processes during time $[s, t)$ are expressed in the bivariate form as $Y(s, t)$.

### B. System Model

As shown in Fig. 1, we consider a multi-user wireless-powered communication system including one AP and $K$ UEs

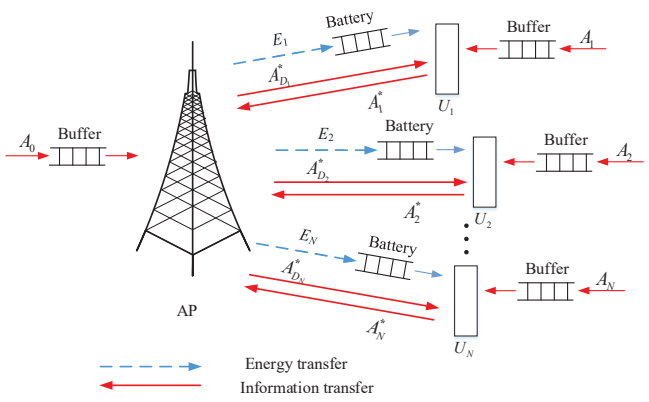


Fig. 1. System model with wireless energy transfer in the downlink and wireless information transmissions in both uplink and downlink

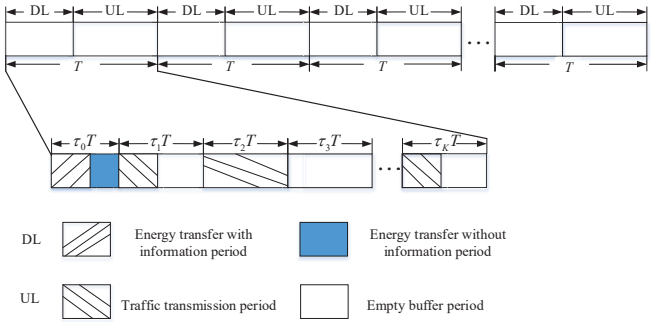


Fig. 2. The time (allocation) model

denoted by $\{U_k, 1 \leq k \leq K\}$ whose locations are fixed. The AP is equipped with $M$ independent antennas and transmits RF signal to the UEs in the DL. The UEs, which are all single-antenna devices, split the energy from the received DL signal into two parts, where one part is used to recover the information and the other part is stored into a battery. In the UL, the stored energy is used to send data from each UE to the AP. Moreover, the system is assumed to work in half-duplex mode.

The time model consists of multiple consecutive time blocks (TBs) which are numbered by $t = 1, 2, \cdots$. Each TB consists of a DL phase and a UL phase. For convenience, the duration of each TB is normalized as 1. The system adopts the harvest-then-transmit protocol [9], as depicted in Fig. 2. The transmission time allocated to the DL and UL during a TB is determined by parameters $\tau = \{\tau_k : 0 \leq k \leq K\}$, where $\sum_{k=0}^{K} \tau_k \leq 1$. In each TB, during the first $\tau_0$ amount of time, AP transfers wireless energy and possibly also data to each UE in the DL. A fixed amount of the harvested energy is used by each UE to recover the information while the remaining energy is stored into the battery to support data transmission in the UL. Thereafter, $\mathrm{U}_k$ $(1 \leq k \leq K)$ is assigned with $\tau_k$ amount of time to conduct UL transmission.

As assumed in the literature, the channel reciprocity holds for the DL and UL which share the same spectrum resource. The channel is quasi-static flat block fading. Specifically, we use $\widetilde{\mathbf{h_k}}(t)$ to denote the small scale channel fading gain between the AP and $U_k$ in the $t$th TB. And $\widetilde{\mathbf{h_k}}(t)$ is assumed to remain constant during each TB but to be independent and identically distributed (i.i.d) over different TBs. Note that $\widetilde{\mathbf{h_k}}(t)$ is a $M$-dimension vector. With the knowledge of channel state information, the system is assumed to adopt maximum ratio transmission (MRT) policy to perform the DL energy and information transfer and maximum ratio combining (MRC) policy to deal with the UL information [12, 13, 22]. Consequently, the total channel power gain holds as $h_k(t) = ||\widetilde{\mathbf{h_k}}(t)||^2$ for the link between the AP and $U_k$ [12, 13]. We highlight that the small scale fading feature used in this paper is general, which can be Rayleigh fading, Nakagami-m fading, Ricean fading and etc. The analysis is always tractable as long as the statistical information of $h_k$ is available.

### C. Energy Harvesting and Data Transmission Rate

The transmission power of each antenna of the AP, denoted by $p_0$, is assumed to be constant. In the $t$th TB, the RF energy harvesting rate of $U_k$ $(1 \leq k \leq K)$ is given by

$$p_{RF_k}(t) = p_0 h_k(t) l_k + N_0 W, \tag{1}$$

where $N_0$ denotes the power spectral density of background noise and $W$ denotes the bandwidth. Besides, $l_k$ denotes the deterministic power gain of path loss which only depends on the distance between $U_k$ and the AP. Typically, in order to guarantee $U_k$ to harvest enough energy to conduct data transmission, the amount of energy harvested from the AP is always much larger than that from the background noise, which implies $N_0 W$ in the righthand side of (1) can be neglected [9]. Therefore, we have

$$p_{RF_k}(t) \approx p_0 h_k(t) l_k. \tag{2}$$

In each TB, fixed level of power, denoted by $p_D$, is used by each UE to perform DL information recovery. Since the signal noise ratio (SNR) of the mixed RF signal is invariant no matter how much energy is used to recover the DL information, the transmission rate from the AP to $U_k$ $(1 \leq k \leq K)$ holds as

$$R_{D_k}(t) = W \log_2(1 + \frac{p_0 h_k(t) l_k}{N_0 W}), \tag{3}$$

Additionally, the remaining RF energy needs to be transferred into the direct-current (DC) energy before the UEs can use it to send data. To characterize the behavior of RF energy harvesting circuit, we adopt a practical non-linear energy harvesting model proposed in [7, 13]. In this model, the energy harvesting rate of $U_k$ $(1 \leq k \leq K)$ is given by [7, 13]

$$p_{DC_k}(t) = \pi \frac{1 - e^{-\nu_1 p_{R_k}(t)}}{1 + e^{-\nu_1 (p_{R_k}(t) - \nu_2)}}, \tag{4}$$

where $p_{R_k}(t) = p_{RF_k}(t) - p_D$ denotes the remaining RF power input to the RF energy harvesting circuit after information recovery. Parameters $\pi$, $\nu_1$ and $\nu_2$ in (4) capture the joint effects of various non-linear phenomena caused by hardware

limitations. More specifically, $\pi$ represents the maximum power that can be harvested by the RF energy harvesting circuit, $\nu_1$ and $\nu_2$ are related to different physical hardware phenomena, such as the circuit sensitivity and current leakage.

We assume, at $U_k$, its harvested energy is mainly consumed by its data transmission, ignoring the other part of its functionalities. Each UE adopts a typical best-effort policy to allocate transmission power for its data transmission. Specifically, the transmission power at $U_k$ in the $t$th TB is given by

$$p_k(t) = \frac{\min\{E_k(t) + p_{DC_k}(t)\tau_0, b\}}{\tau_k}, \tag{5}$$

where $b$ denotes the energy storage capacity of the battery and $E_k(t)$ denotes the amount of remaining energy at the beginning of the $t$th TB. The intuition behind the power allocation policy is to maximize the transmission power through using up the remaining energy and the harvested energy at the end of each TB, such that the data transmission capacity of each UE is maximized in each TB.

Hence, the transmission rate of $U_k$ during the UL phase of the $t$th TB holds as

$$R_k(t) = W \log_2(1 + \frac{p_k(t)h_k(t)l_k}{N_0 W}). \tag{6}$$

### D. Performance Metrics of Interest

Throughout this paper, region $[s, t)$ is used to represent the time from the $s$th TB to the $t$th TB, where we always assume $0 \leq s \leq t$. In order to reduce data backlog or energy storage capacity for the communication nodes in a WPC system, the duration of one TB should be set as short as possible. Therefore, traffic can be assumed to only arrive at the AP or each UE at the beginning of each TB. Besides, we assume the traffic arrival process for each node is i.i.d over different TBs. We use $A_k(s, t)$ $(0 \leq k \leq K)$ to denote the cumulative amount of the traffic arrivals during $[s, t)$. Here, $k$ is used to identify the communication nodes where $k = 0$ represents the AP and $k = 1, \cdots, K$ represents the $k$th UE, i.e., $U_k$. The corresponding departure process of $A_k(0, t)$ is denoted by $A_k^*(0, t)$. It is easily verified that, for a system with input $A_k(t)$ and output $A_k^*(t)$, there holds [23]

$$A_k^*(0, t) = \inf_{0 \leq s \leq t} \{A_k(0, s) + C_k(s, t)\}, \tag{7}$$

where $C_k(s, t)$ represents the cumulative transmission capacity within time $[s, t)$.

This paper focuses on the data transmission performance of the AP in the DL and that of each UE in the UL. At each communication node, the stochastic arrival traffic is stored in the buffer and waits for being served based on first in first out policy. Our focus is on the backlog performance at each communication node. For a node with infinite buffer capacity, its backlog holds as [23]

$$\begin{aligned} Q_k(t) &= A_k(0, t) - A_k^*(0, t) \\ &= A_k(0, t) - \inf_{0 \leq s \leq t} \{A_k(0, s) + C_k(s, t)\} \\ &= \sup_{0 \leq s \leq t} \{A_k(s, t) + C_k(s, t)\} \end{aligned}, \tag{8}$$

where $Q_k(t)$ denotes the backlog for an infinite-capacity buffer in the $t$th TB. In this paper, we take finite buffer capacity into account. The backlog of $U_k$ in the $t$th TB is denoted by $B_k(t)$ and $B_k(t) \equiv 0$ when $t = 0$. It is easily verified that $B_k$ is upper-bounded by $Q_k$ due to packet loss, there holds

$$B_k(t) \leq \sup_{0 \leq s \leq t} \{A_k(s, t) + C_k(s, t)\}. \tag{9}$$

The buffer constraint is defined as

$$Pr\{B_k(t) > x_k\} \leq \epsilon_k, \tag{10}$$

where $x_k$ denotes the buffer capacity. The buffer constraint means the buffer overflow probability should be control within $\epsilon_k$ for a node with buffer capacity $x_k$.

In this paper, we study the throughput performance based on the buffer constraint, which is called as the *buffer-constrained throughput*, representing the maximum traffic rate that the AP or $U_k$ can sustain to meet the buffer constraint:

$$r_k^{\max} = \sup\{r_k : Pr\{B_k(t) > x_k\} \leq \epsilon_k\}, \tag{11}$$

where $r_k$ denotes the traffic arrival rate. Compared to the conventional throughput characterized by the instantaneous capacity or ergodic capacity, the buffer-constrained throughput is not only associated with system service process, but also depends on the traffic characteristics and buffer overflow probability requirement.

## III. Performance Analysis

### A. System Service Characterization

According to definitions (9), the backlog performance are both related to the cumulative transmission capacity $C_k(s, t)$. At time region $(0, t)$, $C_k$ is given by

$$C_k(0, t) = \sum_{i=1}^{t} R_k(i)\tau_k, \tag{12}$$

where $R_k(i)$ denotes the transmission rate in the $i$th TB. When $1 \leq k \leq K$, $C_k(0, t)$ represents the service process of $U_k$. In this case, $R_k(i)$ is deterministic within a TB and can be obtained from (6). When $k = 0$, $C_0(0, t)$ represents the service process of the AP. As the AP may send data to different UEs at different time during a TB, according to (3), the transmission rate $R_0(i)$ varies with the selection of UE to communication with. Thus, $R_0(i)$ is no longer deterministic during a TB but a complex random variable which is always equal to one of the elements from set $\{R_{D_k}(i) : 1 \leq k \leq K\}$, where $R_{D_k}(i)$ is obtained from (3).

### B. Buffer Overflow Probability

The following lemmas provides general expression of buffer overflow probability with respect to buffer capacity.

**Lemma 1.** *Consider a stable WPC system as depicted in Fig. 1, where the data transmission capacity and the traffic arrival process of a node is characterized as $C_k$ and $A_k$ respectively. If $C_k$ and $A_k$ are independent of each other and*

*both i.i.d processes, then for a given buffer capacity $x_k$, the corresponding buffer overflow probability is bounded by*

$$Pr\{B_k(t) > x_k\} \leq e^{-\theta_k x_k},$$

*for some $\theta_k > 0$ which meets $\mathbb{E}[e^{\theta_k A_k(0,1)}]\mathbb{E}[e^{-\theta_k C_k(0,1)}] \leq 1$.*

*Proof:* Please see Appendix A. ■

In Lemma 1, the condition $\mathbb{E}[e^{\theta_k A_k(0,1)}]\mathbb{E}[e^{-\theta_k C_k(0,1)}] \leq 1$ implies a sufficient stability condition for a system [23]

$$\begin{aligned} \frac{\ln \mathbb{E}[e^{\theta_k A_k(0,1)}]}{\theta_k} &\leq -\frac{\ln \mathbb{E}[e^{-\theta_k C_k(0,1)}]}{\theta_k} \\ \Updownarrow & \\ \lim_{t\to\infty} \frac{\ln \mathbb{E}[e^{\theta_k A_k(0,t)}]}{\theta_k t} &\leq -\lim_{t\to\infty} \frac{\ln \mathbb{E}[e^{-\theta_k C_k(0,t)}]}{\theta_k t} \end{aligned}, \quad (13)$$

where $\frac{\ln \mathbb{E}[e^{\theta_k A_k(0,t)}]}{\theta_k}$ and $-\frac{\ln \mathbb{E}[e^{-\theta_k C_k(0,t)}]}{\theta_k}$ represent the statistical envelops of processes $A_k$ and $C_k$ respectively [23, 24]. And, $\alpha_{\theta_k} \triangleq \frac{\ln \mathbb{E}[e^{\theta_k A_k(0,1)}]}{\theta_k}$ and $\beta_{\theta_k} \triangleq -\frac{\ln \mathbb{E}[e^{-\theta_k C_k(0,1)}]}{\theta_k}$ denote the corresponding envelop rates respectively.

Note that a variety of traffic can be characterized by $\alpha_\theta$, including Poisson traffic, on-off traffic, self-similar traffic and heavy-tail traffic [23]. Specially, a typical periodical Poisson traffic can be described as follows [25]

$$\alpha_\theta = \frac{\ln \mathbb{E}[e^{\theta A(0,1)}]}{\theta} = \frac{\lambda}{\theta}(e^{\theta L} - 1). \quad (14)$$

Here, $\lambda$ denotes the mean number of the arrival packets during each TB, $L$ denotes the constant packet size.

Additionally, $C_k$ is i.i.d process if and only if $R_k(t)$ is i.i.d over time. On one hand, when $k = 0$, the instantaneous transmission rate depends on the selection of UE to communication with, which is reflected by the traffic characteristics. Besides, the traffic arrival process of the AP and the channel power gain for each UE are both i.i.d. Hence, $R_k(t)$ satisfies i.i.d property according to (3). On the other hand, when $1 \leq k \leq K$, $R_k(t)$ not only depends on the channel power gain but also the amount of energy storage $E_k(t)$ at the beginning of the $t$th TB according to (5) and (6). It is easily verified that $E_k(t)$ depends on both the energy harvesting and data transmission before the $t$th TB. Therefore, $R_k(t)$ dose not meet the i.i.d property in this case. However, a lower bound of $R_k(t)$, which ignores the impact of $E_k(t)$, is still i.i.d and able to guarantee the lower bound of the performance of each UE. We remark that this lower bound is accurate since $E_k(t) \approx 0$ $(t \geq 0)$ is reasonable in a WPC system from the economic point of view. Specifically, the transmission power of the AP and the energy storages capacity of each UE can be configured as small as possible with appropriate time allocation and the statistical information of traffic arrivals, which will be studied in the subsequent section. Therefore, the stored energy is almost used up by each UE at the end of each TB. In summary, the cumulative transmission capacity $C_k$ can be approximately considered as i.i.d process. And we let

$$\begin{aligned} \beta_{\theta_k} &= \lim_{t\to\infty} -\frac{\ln \mathbb{E}[e^{-\theta_k C_k(0,t)}]}{\theta_k t} \\ &= \lim_{t\to\infty} -\frac{\ln \mathbb{E}[e^{-\theta_k \sum_{i=1}^{t} R_k(i)\tau_k}]}{\theta_k t} \\ &\approx \lim_{t\to\infty} -\frac{\sum_{i=1}^{t} \ln \mathbb{E}[e^{-\theta_k R_k \tau_k}]}{\theta_k t} \\ &= -\frac{\ln \mathbb{E}[e^{-\theta_k R_k \tau_k}]}{\theta_k} \end{aligned}. \quad (15)$$

Here we omit the identification of TB $i$ in random variable $R_k$ for simplification, since $R_k$ is i.i.d over different TBs. Note that $\beta_{\theta_k}$ is available as long as $R_k$ is light-tailed distributed [26]. In fact, for various typical fading channels, such as Rayleigh, Rice, Nakagami-m, Weibull, and lognormal fading channels, the distribution of $R_k$ has been proved to own light-tailed property [26].

Additionally, according to Lemma 1, the buffer overflow probability decreases as $\theta_k$ increases, which means a tighter bound would be achieved with a larger $\theta_k$. However, $\theta_k$ is constrained by (13), i.e.,

$$\alpha_{\theta_k} \leq \beta_{\theta_k} \quad (16)$$

for both DL and UL data transmissions. Hence, the optimal $\theta_k$ can be found out according to the following expression,

$$\theta_k^{opt} = \max\{\theta_k : \alpha_{\theta_k} \leq \beta_{\theta_k}\} \quad . \quad (17)$$

With Lemma 1, the buffer overflow probability of the DL and that of the UL can be analyzed specifically. The following theorems summarize the obtained bounds.

**Theorem 1.** *For the DL transmission of the AP (i.e., $k = 0$) or the UL transmission of the $U_k$ (i.e. $1 \leq k \leq K$), with buffer capacity $x_k$, the buffer overflow probability is upper bounded by*

$$Pr\{B_k(t) > x_k\} \leq e^{-\theta_k x_k}.$$

*Here, for system stability, $\theta_k$ should meet $\alpha_{\theta_k} \leq \beta_{\theta_k}$, where $\alpha_{\theta_k}$ and $\beta_{\theta_k}$ are the envelop rate of traffic arrival and transmission capacity at the AP or $U_k$ respectively. There holds,*

$$\alpha_{\theta_k} = \frac{\ln \mathbb{E}[e^{\theta_k A_k(0,1)}]}{\theta_k}. \quad (18)$$

$$\beta_{\theta_k} = \begin{cases} -\frac{\ln \sum_{k=1}^{K} \mathbb{E}[e^{-\theta_0 R_{D_k} \tau_0}] Pr\{k\}}{\theta_k}, & k = 0 \\ -\frac{\ln \mathbb{E}[e^{-\theta_k R_k \tau_k}]}{\theta_k}, & 1 \leq k \leq K \end{cases}, \quad (19)$$

*where $Pr\{k\}$ denotes the probability that the data being sent by the AP is towards $U_k$, and $\sum_{k=1}^{K} Pr\{k\} = 1$.*

*Proof:* Please see Appendix B. ■

### C. Buffer-Constrained Throughput

With the information of the buffer constraint including backlog capacity $x_k$ and buffer overflow probability $\epsilon_k$, the maximum sustained throughput of the input traffic, i.e., the buffer-constrained throughput, can be derived.

**Theorem 2.** *For the DL transmission of the AP (i.e., $k = 0$) or the UL transmission of the $U_k$ (i.e. $1 \leq k \leq K$) with buffer constraint $(x_k, \epsilon_k)$, the buffer-constrained throughput of the input traffic holds as*

$$r_k^{\max} = g_k^{-1}(\beta_{-\frac{\ln \epsilon_k}{x_k}}),$$

*where $g_k^{-1}(\alpha_{\theta_k})$ denotes the inverse function of $g_k(r_k) = \alpha_{\theta_k}$ and $\theta_k = -\frac{\ln \epsilon_k}{x_k}$.*

*Proof:* Please see Appendix C. ■

Note that for Poison traffic, $g_k(r_k) = \frac{r_k}{\theta_k L_k}(e^{\theta_k L_k} - 1)$ according to (14), where $r_k = \lambda_k L_k$. Therefore, the buffer-constrained throughput holds as

$$r_k = \frac{\alpha_{\theta_k}\theta_k L_k}{e^{\theta_k L_k} - 1} = -\frac{\beta_{-\frac{\ln \epsilon_k}{x_k}} \frac{\ln \epsilon_k}{x_k} L_k}{e^{-\frac{\ln \epsilon_k}{x_k} L_k} - 1}. \tag{20}$$

In Theorem 2, $\theta_k = -\frac{\ln \epsilon_k}{x_k}$ decreases as $x_k$ or $\epsilon_k$ increases. Besides, it is easily verified that $\beta_{\theta_k}$ is a decreasing function with respect to $\theta_k$ and $g_k(r_k)$ is an increasing function with respect to $r_k$. Therefore, the communication node with looser buffer constraint is able to sustain higher traffic arrival rate. Furthermore, when the buffer constraint is loosen infinitely, i.e., $x_k \to \infty$ or $\epsilon_k \to 1$, there holds $\theta_k \to 0$. At this time, $\beta_{\theta_k}$ converges to the mean channel capacity $R_k\tau_k$ $(0 \leq k \leq K)$ and $\alpha_{\theta_k}$ converges to the mean traffic arrival rate $r_k$ [23]. Further according to the stability condition, we conclude that $r_k$ converges to the mean channel capacity $R_k\tau_k$ when buffer constraint is loosen infinitely.

## IV. Resource Allocation Study

### A. DL Transmission Power And Energy Storage Capacity

Due to the reason that the DL transmission power of the AP $p_0$ has a great difference on both DL and UL transmissions, it is advisable to adjust $p_0$ to guarantee the performance requirements for all the communication nodes. The following theorem introduces the analytical approach to find out the minimum $p_0$.

**Theorem 3.** *Suppose the traffic arrival process of the AP and $U_k$ $(0 \leq k \leq K)$ is characterized by envelop rate $\alpha_{\theta_k} = g_k(r_k)$, the time allocation policy is fixed as $\{\tau_k : 0 \leq k \leq K\}$ and the energy storage capacity is sufficient. If the buffer constraint is given as $(x_k, \epsilon_k)$, the required minimum DL transmission power $p_0^{\min}$ holds as*

$$p_0^{\min} = \max\{p_{0,k} : 0 \leq k \leq K\}.$$

*Here, $p_{0,0}$ is the solution of the following equation*

$$\sum_{k=1}^{K} \mathbb{E}[e^{\frac{\ln \epsilon_0}{x_0} W \log_2(1+\frac{p_0 h_k l_k}{N_0 W})\tau_0}] Pr\{k\} = e^{\frac{\ln \epsilon_0}{x_0} g_0(r_0)}.$$

*$p_{0,k}$ $(1 \leq k \leq K)$ is the solution of the following equation*

$$\mathbb{E}[e^{\frac{\ln \epsilon_k}{x_k} W \log_2(1+\frac{\pi_k \frac{1-e^{-\nu_1(p_0 h_k l_k - p_D)}}{1+e^{-\nu_1(p_0 h_k l_k - p_D - \nu_2)}} \tau_0 h_k l_k}{\tau_k N_0 W})\tau_k}] = e^{\frac{\ln \epsilon_k}{x_k} g_k(r_k)}$$

*Proof:* Please see Appendix D. ■

Note that $p_0^{\min}$ may not be available in closed-form when the channel power gain is random over time. However, it can be analyzed with the help of some mathematical calculation tools like MATLAB. Also, $p_0^{\min}$ is achieved provided that the energy storage capacity of each UE is large enough. However, large energy storage capacity may lead to high economic cost while small energy storage capacity restricts the UL performance of the UEs. It is consequently worth finding out the energy storage capacity as small as possible to ensure the UL performance requirements.

**Theorem 4.** *Suppose the conditions are all the same as introduced in Theorem 3, the required minimum energy storage capacity $b_k^{\min}$ $(1 \leq k \leq K)$ can be ascertained by solving the following equation,*

$$\mathbb{E}[e^{\frac{\ln \epsilon_k}{x_k} W \log_2(1+\frac{b_k^{\min} h_k l_k}{\tau_k N_0 W})\tau_k}] = e^{\frac{\ln \epsilon_k}{x_k} g_k(r_k)}.$$

*Proof:* The proof is similar with that of Theorem 3. We only need to replace the transmission power $p_k$ with $\frac{b_k^{\min}}{\tau_k}$ in (26), due to the reason that $\frac{b_k^{\min}}{\tau_k} \geq p_k$. ■

### B. Time Allocation Scheme

In the considered WPC system, the UEs suffer two times of path loss during each TB, where one is in DL energy transfer and the other is in UL information transmission. This phenomenon which causes severe performance degradation is called as the doubly near-far problem [9]. In this section, we are going to find out the optimal time allocation scheme to maximize the minimum individual throughput at each UE under the given buffer constraint $(x, \epsilon)$. The problem is also known as max-min problem [7], which is given as follows

$$\begin{aligned} &\max\ r \\ &s.t.\quad r_k \geq r,\ 1 \leq k \leq K \\ &\qquad \sum_{k=0}^{K} \tau_k \leq 1 \\ &\qquad Pr\{B_k(t) > x\} \leq \epsilon \end{aligned}, \tag{21}$$

where $r_k$ is the buffer-constrained throughput of $U_k$. For convenience, we call this maximum individual throughput as the *max-identical throughput*. Note that the max-identical throughput in this paper differs from another ones studied in the literature on the consideration of buffer constraint. For example, in [9], the max-identical throughput called as "common throughput" is derived as the maximum mean channel capacity which can be guaranteed by each UE simultaneously. We highlight that our max-identical throughput converges to the common throughput of [9] by loosening the buffer constraint

infinitely. The reason is that when $x_k \to \infty$ or $\epsilon_k \to 1$, $r_k$ converges to the mean channel capacity of $R_k\tau_k$.

According to Theorem 2, $r_k$ can be related to the transmission capacity envelop rate by $g_k^{-1}(\beta_{-\frac{\ln\epsilon}{x}})$, where $g_k^{-1}(\beta)$ is a monotonically increasing function of $\beta$. Besides, $\beta_{-\frac{\ln\epsilon}{x}}$ is a monotonically increasing function of $R_k\tau_k$ according to (19), and $R_k\tau_k$ is a monotonically increasing function of both $\tau_0$ and $\tau_k$ according to (5) and (6). Therefore, $r_k$ is consequently a monotonically increasing function of both $\tau_0$ and $\tau_k$. Hence, the optimal time allocation solution $\tau^{opt}$ should satisfy $\sum_{k=0}^{K}\tau_k = 1$. Otherwise the remaining available time can be allocated to each UE such that $r$ can still be improved. Additionally, problem (21) is designed to maximize the traffic throughput of the UE with the worst channel condition, e.g. the largest distance far from the AP. The optimal time allocation solution $\tau^{opt}$ should allocate the same throughput to all the UEs. Otherwise, the UEs whose throughput is higher than $r$ can give some time to the other UEs to increase $r$. Additionally, as the buffer constraint is fixed as $(x,\epsilon)$, the optimal parameter $\theta$ is always equal to $-\frac{\ln\epsilon}{x}$ according to Theorem 1 and (17). Consequently, the max-min problem is transformed to the following optimization problem,

$$\begin{aligned} \max\ & r \\ s.t.\quad & r_k = r,\ 1 \le k \le K \\ & \sum_{k=0}^{K}\tau_k = 1 \\ & \theta = -\frac{\ln\epsilon}{x} \end{aligned} \quad . \tag{22}$$

In order to find out the optimal time allocation solution for problem (22), we first focus on the following problem where $\tau_0$ is given.

$$\begin{aligned} \text{find}\quad & \tau^* \text{ and } r \\ s.t.\quad & r_k = r,\ 1 \le k \le K \\ & \sum_{k=1}^{K}\tau_k = 1-\tau_0 \\ & \theta = -\frac{\ln\epsilon}{x} \end{aligned} \quad . \tag{23}$$

Here, we call $r$ as the *identical throughput*.

Without loss of generality, we assume $U_1$ has the best mean channel condition among all the UEs. In what follows, we propose a dichotomy-based algorithm to find out $\tau^*$ and $r$ for problem (23).

In step 1 of Algorithm 1, we set $\tau_1^{\min} = 0$ and $\tau_1^{\max} = \frac{1-\tau_0}{K}$ in order to let $\upsilon^{\min} > 0$ and $\upsilon^{\max} < 0$, such that the dichotomy approach can be started. Here, we set the maximum $\tau_1$ as $\frac{1-\tau_0}{K}$ due to the reason that the transmission time of $U_1$ is always less than the mean remaining time for each UE since $U_1$ is in the best channel condition. When $\tau_0$ and $\tau_1$ is fixed, the buffer-constrained throughput of $U_1$, denoted by $r_1$, can be ascertained according to Theorem 1 and Theorem 2. In steps 3, 5 and 9, $\tau_k$ can be obtained as the solution of equation $r_k = r_1$, where $r_1 = [r_1^{\min},\ r_1^{\max},\ r_1^h]$ respectively. As $r_k$ monotonically increases with $\tau_k$, the equation $r_k = r_1$ has only one solution for given $\tau_0$ and $\tau_1$. In step 4, $\upsilon^{\min} > 0$ means there is available remaining time which can be allocated to the UEs, i.e., $\tau_1$ should be increased. In step 6, $\upsilon^{\max} < 0$ means the total amount of time which should be allocated to the UEs is more than the maximum amount $1-\tau_0$, i.e., $\tau_1$ should be decreased. Steps 7-22 are the dichotomy approach to find out $\tau^*$ to meet the conditions of problem (23).

**Algorithm 1** Solution of problem (23)

1: **initialize** $\tau_1^{\min} = 0$ and $\tau_1^{\max} = \frac{1-\tau_0}{K}$;
2: compute the buffer-constrained throughput $r_1^{\min}$;
3: find out $\tau^{\min}$ subject to $r_k = r_1^{\min}$ for all $k = 2, \cdots, K$;
4: $\upsilon^{\min} = 1 - \sum_{k=0}^{K}\tau_k^{\min}$;
5: compute $r_1^{\max}$ and find out $\tau^{\max}$ with respect to $\tau_1^{\max}$;
6: $\upsilon^{\max} = 1 - \sum_{k=0}^{K}\tau_k^{\max}$;
7: **repeat**
8: set middle point $\tau_1^h = \frac{\tau_1^{\min}+\tau_1^{\max}}{2}$;
9: compute $r_1^h$ and find out $\tau^h$ with respect to $\tau_1^h$;
10: $\upsilon^h = 1 - \sum_{k=0}^{K}\tau_k^h$;
11: **if** $\upsilon^h < 0$ **then**
12: $\tau_1^{\max} = \tau_1^h$, $\upsilon^{\max} = \upsilon^h$, then go to step 16;
13: **else**
14: $\tau_1^{\min} = \tau_1^h$, $\upsilon^{\min} = \upsilon^h$, then go to step 16;
15: **end if**
16: **until** $\upsilon^{\min}\upsilon^{\max} == 0$ or $\tau^{\max} - \tau^{\min} \le \varphi$, where $\varphi$ denotes the precision requirement.
17: **if** $\upsilon^{\min} == 0$ or $\upsilon^{\max} == 0$ **then**;
18: $\tau_1 = \tau^{\min}$ or $\tau_1 = \tau^{\max}$;
19: **else**
20: $\tau_1 = \frac{\tau_1^{\min}+\tau_1^{\max}}{2}$;
21: **end if**
22: compute $r = r_1$ with $\tau_1$ and find out $\tau^*$ subject to $r_k = r_1$.

In step 1 of Algorithm 1, we set $\tau_1^{\min} = 0$ and $\tau_1^{\max} = \frac{1-\tau_0}{K}$ in order to let $\upsilon^{\min} > 0$ and $\upsilon^{\max} < 0$, such that the dichotomy approach can be started. Here, we set the maximum $\tau_1$ as $\frac{1-\tau_0}{K}$ due to the reason that the transmission time of $U_1$ is always less than the mean remaining time for each UE since $U_1$ is in the best channel condition. When $\tau_0$ and $\tau_1$ is fixed, the buffer-constrained throughput of $U_1$, denoted by $r_1$, can be ascertained according to Theorem 1 and Theorem 2. In steps 3, 5 and 9, $\tau_k$ can be obtained as the solution of equation $r_k = r_1$, where $r_1 = [r_1^{\min},\ r_1^{\max},\ r_1^h]$ respectively. As $r_k$ monotonically increases with $\tau_k$, the equation $r_k = r_1$ has only one solution for given $\tau_0$ and $\tau_1$. In step 4, $\upsilon^{\min} > 0$ means there is available remaining time which can be allocated to the UEs, i.e., $\tau_1$ should be increased. In step 6, $\upsilon^{\max} < 0$ means the total amount of time which should be allocated to the UEs is more than the maximum amount $1-\tau_0$, i.e., $\tau_1$ should be decreased. Steps 7-22 are the dichotomy approach to find out $\tau^*$ to meet the conditions of problem (23).

The optimal time solution $\tau^{opt}$ and the max-identical throughput can be further obtained through one-dimensional search after problem (23) is solved. Specifically, if the value of $\tau_0$ is set from 0 to 1 with step length $\omega$, we can obtain $\lfloor\frac{1}{\omega}\rfloor$ results of time allocation solution and the corresponding identical throughput for different $\tau_0$. The the max-identical throughput and the optimal time allocation solution of problem (22) can be obtained by choosing the maximum $r$ and the corresponding $\tau^*$ among the $\lfloor\frac{1}{\omega}\rfloor$ results. The solution of problem (22) is summarized as the following algorithm.

**Algorithm 2** Solution of max-min problem (22)

1: **initialize** $\tau_0$=0, step length $\omega$, $r^{max} = 0$, $\tau^{\text{opt}} = []$;
2: **repeat**
3: apply Algorithm 1 to obtain $r$ and $\tau^*$;
4: **if** $r > r^{max}$ **then**
5: $r^{max} = r$, $\tau^{\text{opt}} = \tau^*$;
6: **end if**
7: $\tau_0 = \tau_0 + \omega$;
8: **until** $\tau_0 \ge 1$

In Algorithm 2, the accuracy of the solution depends on the step length $\omega$. Concretely, the smaller $\omega$ is, the more accurate

solution we can obtain. On the other hand, the duration of a TB cannot be too long due to the economic cost constraint on data buffer capacity and energy storage capacity. Actually, the subsequent numerical result verifies that the throughput result with $\omega = 0.01$ is already as accurate as that with $\omega = 0.0001$ when the duration of a TB is 1s. In the end, the calculation complexity of solving the max-min problem (22) is summarized in the following proposition.

**Proposition 1.** *The calculation complexity of finding out the optimal time allocation solution and max-identical throughput is* $O(\frac{(K-1)\log_2(\frac{1}{K\psi})\log_2(\frac{1}{\psi})}{\omega})$.

*Proof:* Firstly, the calculation complexity of Algorithm 1 depends on the precision of $\tau^*$, which is denoted by $\psi$. It is easily verified that the calculation complexity of solving $\tau_1$ is upper-bounded by $\log_2(\frac{1}{K\psi})$ while that of solving $\tau_k$ $(2 \leq k \leq K)$ is upper-bounded by $\log_2(\frac{1}{\psi})$. Thus, the calculation complexity of Algorithm 1 holds as $O((K-1)\log_2(\frac{1}{K\psi})\log_2(\frac{1}{\psi}))$. Secondly, the calculation complexity of the one-dimensional search in Algorithm 2 is $O(\frac{1}{\omega})$. Therefore, the overall calculation complexity of solving problem (22) holds as $O(\frac{(K-1)\log_2(\frac{1}{K\psi})\log_2(\frac{1}{\psi})}{\omega})$. ■

## V. Results

In this section, we present numerical results from the analysis to discuss the performance of the WPC system. If not otherwise highlighted, the various involved parameters and the adopted analysis scenarios are as follows. The AP has equal probability to send data to each UE, i.e., $Pr\{k\} = \frac{1}{K}$. We assume identical configurations and traffic load for each UE. The energy harvesting parameters are set as $\pi = 0.01$mW, $v_1 = 47.083 \times 10^3$ and $v_2 = 0.0029$mW [13]. The power used to recover the DL information at each UE is fixed as $p_D = -60$dBm. The buffer capacity and the maximum tolerable buffer overflow probability are set to $x_k = 20$ packets and $\epsilon_k = 10^{-4}$ $(1 \leq k \leq K)$ respectively. The number of UEs is set to $K = 2$. The time allocation parameter is assumed to be $\tau = (0.2, 0.4, 0.4)$. The transmission power of AP is set to $p_0 = 30$dBm (i.e., 1W) and the duration of a TB is 1s. In order to study the performance for the stochastic traffic which is served on stochastic channel, we assume the number of packets periodically arriving at each communication node follows Poisson distribution and the packet size is fixed as 100kbits. The traffic envelop rate can be referred in (14). For the channel model, we set the bandwidth $W = 1$MHz and the power spectral density of the background noise $N_0 = -130$dBm/Hz. The number of antennas of the AP is set to $M = 8$. The links of the antennas are all i.i.d Nakagami-2 fading with mean 1. Thus, the channel power gain $h$ follows Gamma distribution with shaper parameter $m = 16$ and rate parameter $\mu = 2$ [27]. Additionally, the path loss is assumed to be $l_k = \rho_k^{-2}$ with 30dB power attenuation at a reference distance of 1m, where $\rho_k = \frac{10k}{K}$ (meters) denotes the distances between the AP and $U_k$ [9]. For a two-user scenario, there holds $\rho = [5, 10]$m.

Fig. 3 depicts buffer overflow probability varying with buffer capacity. The mean arrival rate of the AP and that of each UE

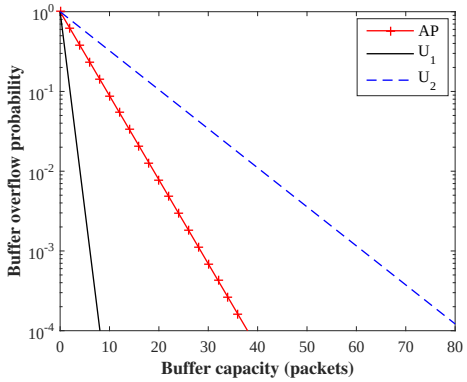


Fig. 3. Buffer overflow probability

are set to $\lambda_0 = 30$ and $\lambda_k = 8$ $(1 \leq k \leq 2)$ packets per TB, respectively. It is observed that the buffer overflow probability is an exponentially decreasing function with respect to the buffer capacity. Besides, the backlog performance of $U_1$ is much better than that of $U_2$. This implies $\lambda_k$ is light load for $U_1$ but heavy load for $U_2$, since $U_1$ is closer to the AP. On the other hand, Fig. 3 reminds the buffer capacity should be carefully determined due to the reason that the number of backlogged packets may be larger than the arrival rate within a non-ignorable probability (e.g. $10^{-4}$). Particularly, $U_2$ needs large buffer to guarantee the buffer overflow probability for the heavy-load traffic. However, the buffer capacity of the WPC devices cannot be as large as the traditional communication nodes jointly due to their small sizes and economic cost constraint. Hence, traffic access control and resource allocation are rather important for WPC devices.

In Fig. 4, the buffer-constrained throughput performance is depicted for the AP, $U_1$, and $U_2$ respectively. We can easily analyze how much traffic be sustained by a communication node under given buffer constraints. Fig. 4 indicates the traffic throughput can be improved by loosening the buffer constraint, i.e., increasing the buffer capacity or the tolerable buffer overflow probability. On the other hand, the increasing rate of throughput becomes smooth when either buffer capacity or buffer overflow probability is sufficiently large (i.e., $x_k > 40$ or $\epsilon_k > 0.1$). As discussed in Section III-C, the throughput will converge to the mean channel capacity if buffer constraint is loosened infinitely. Besides, the throughput performance of AP is the best of the three nodes among which $U_1$ outperforms $U_2$. The reason is due to the doubly near-far phenomenon where the UEs has to suffer the two times of path loss [9].

In Fig. 5, the maximum sustained traffic throughput and the mean channel capacity are depicted. It is well known larger channel capacity can sustained higher traffic throughput. A remarkable gap can be observed between the throughput and the corresponding channel capacity while enforcing non-ignorable buffer constraint into a communication node. The gap increases as the DL transmission power $p_0$ increases. Implied by Fig. 5, if buffer constraint is required in data transmission, using the mean channel capacity would easily lead to overestimation in traffic access control. Besides, the

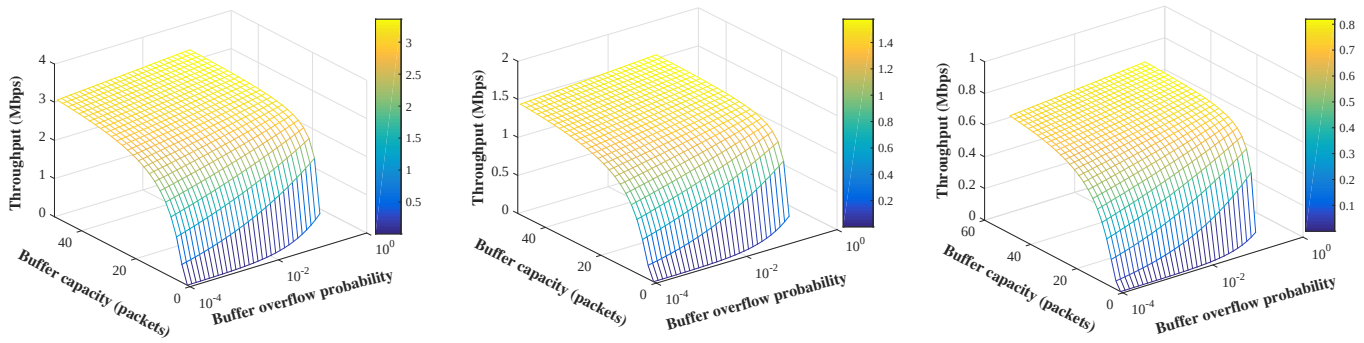


(a) AP (b) $U_1$ (c) $U_2$

Fig. 4. Buffer-constrained throughput

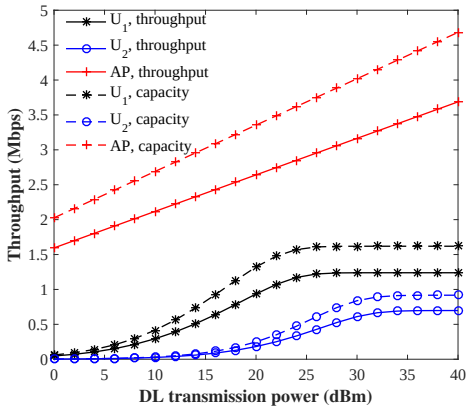


Fig. 5. Buffer-constrained throughput v.s. mean channel capacity

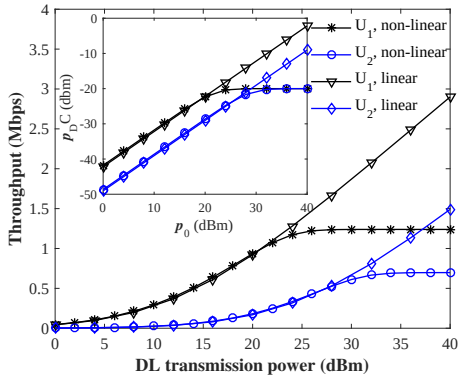


Fig. 6. Buffer-constrained throughput based on different energy harvesting models

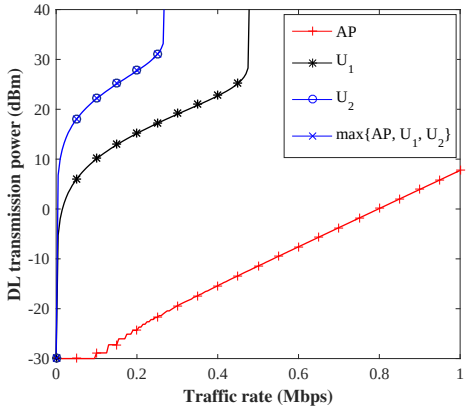


Fig. 7. Minimum DL transmission power required by different traffic rates

throughput and capacity performance always increases with $p_0$ at AP while it converges to a constant at the UEs when $p_0$ is sufficiently large (e.g., $p_0 = 30$dBm at $U_1$). The reason is that the channel capacity increases with its transmission power and $p_0$ is exactly the transmission power of AP. However, the energy harvesting rate is limited by the circuit parameter $\pi$ in terms of the non-linear energy harvesting model (4), which limits maximum transmission power of each UE according to (5). Hence, traffic throughput cannot be increased infinitely for the UEs.

Fig. 6 compares the non-linear energy harvesting model with the typical linear energy harvesting model which is widely used in the literature (e.g., [9–12]). The linear energy harvesting model is expressed as $p_{DC_k} = \eta(p_{RF_k} - p_D)$, where $\eta = 0.1$ is the fixed energy harvesting efficiency [13]. From the subfig, we verify that the energy harvesting rate of non-linear model is upper-bounded by $\pi$. The difference between these two model is that the throughput based on the non-linear model has an upper bound while that based on the linear model dose not. Interestingly, the throughput performance based on the non-linear model agrees with that based on the linear model when $p_0$ is small (e.g., $p_0 < 25$dBm at $U_2$). The observation in Fig. 6 implies that the linear model still performs well in low power regime but may lead to severe overestimate when $p_0$ is sufficiently large.

Fig. 7 and Fig. 8 study the resource allocation policy in the area of DL transmission power and battery capacity. The minimum DL transmission power required to ensure the transmission performance of each node is depicted in Fig.

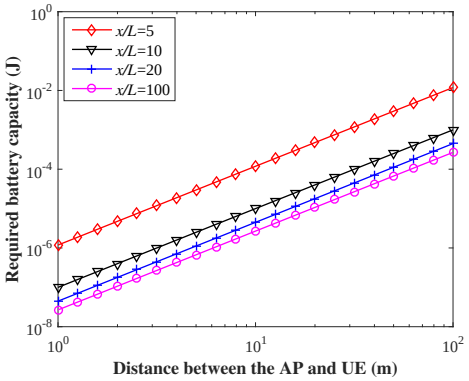


Fig. 8. Battery capacity required under buffer and distance constraints.

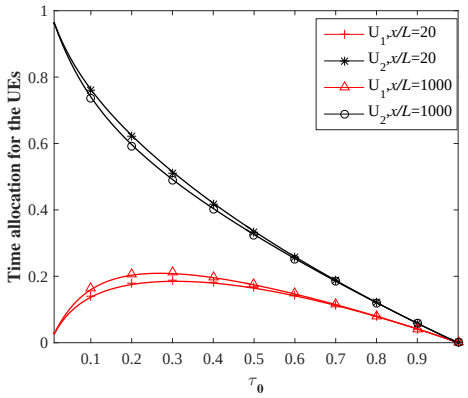


Fig. 10. Time allocation scheme for identical throughput

7. The abscissa describes the traffic rate of the UEs and 40dBm in the ordinate is considered as infinite power. For a practical system, the AP usually sustains higher traffic rate and backlogs more packets than the UEs. In order to reflect this feature, we assume the rate and the buffer capacity of the AP are both twice as much as the UEs. It is shown that the UEs especially $U_2$ require much higher power than the AP to begin data transmission due to the impact of two times of path loss. The system cannot increase the traffic throughput infinitely through rising the transmission power if other conditions are invariant, since the energy harvesting rate is limited by parameter $\pi$. However, if we assume the energy harvesting rate is always sufficient, battery capacity will be a key factor to guarantee the throughput performance. Fig. 8 depicts the impacts of the buffer capacity and the data transmission distance on the minimum battery capacity required to guarantee the throughput performance. It is observed that the required battery capacity is sensitive to the distance between the AP and the UE. The relationship between the battery capacity and the distance follows logarithmical linearity. Besides, stricter buffer constraint requires larger battery capacity. This is because stricter buffer constraint implies higher buffer-constrained throughput needed, which further demands larger amount of minimum energy stored for the UL transmission. However, when loosening the buffer constraint to $x/L = 20$ packets, the required battery capacity is already close to the case where $x/L = 100$ packets. Therefore, from the economic point of view, the tradeoff between the buffer capacity and battery capacity should be carefully taken into account since a small buffer capacity may be able to ensure the battery capacity approach to the convergent minimum value.

Fig. 9 verifies max-min problem (22) is successfully solved. Firstly, Fig. 9(a) presents the identical throughput results obtained by applying Algorithm 1 and Algorithm 2 under different wireless charging time and step lengths. It is observed that the max-identical throughput is sufficiently accurate even with a large step length (i.e., $\omega = 0.1$). Therefore, the search times in Algorithm 2 can be controlled within a small value.

To further study the impacts of buffer constraint on the identical throughput, Fig. 9(b) and Fig. 9(c) are presented. In Fig. 9(b), the identical throughput is achieved with a strict buffer capacity requirement. The optimal time allocation scheme to achieve the max-identical throughput may not be able to maximize the mean channel capacity of the UE at the same time. Fig. 9(b) shows that the identical throughput is lower than the channel capacity of each UE. Besides, the capacities of the UEs are different, where $U_2$ has larger channel capacity than $U_1$, even though $U_2$ suffers worse pass loss and lower transmission power according to (5). It can be explained that the transmission time $\tau_k$ plays an important role in the mean channel capacity of the $U_k$ since the transmission rate of $U_2$ is lower than that of $U_1$. In other words, the mean channel capacity of a UE can be improved by increasing its transmission time when other conditions are invariant. On the other hand, Fig. 9(c) depicts the identical throughput with a loose buffer capacity requirement which is considered as infinite loose buffer constraint. In this case, the buffer-constrained throughput converges to the channel capacity as discussed in Fig. 4. Thus, the max-identical throughput in this case is equivalent to the "common throughput" in [9]. In addition, the optimal time allocation solution without buffer constraint is confirmed to be different from the one taking the buffer constraint into account. Therefore the time allocation policy to guarantee identical transmission capacity among the UEs is not able to guarantee the practical identical traffic throughput while buffer constraint is enforced.

The difference of the time allocation solution between these tow cases is depicted in Fig. 10. It is observed that when $\tau_0 > 0.7$, which is considered as a sufficient long wireless charging time, the time allocation solution to the UE transmission has nothing to do with the buffer constraint. In this case, the channel capacity results in Fig. 9(b) and and those in Fig. 9(c) are identical. In contrast, if the AP just charges the UEs with a small time during each TB, the time allocation solution is dominated by the buffer constraint.

In Fig. 11, the impacts of the number of UEs $K$ on the max-identical throughput is presented. As shown in Fig. 11(a), there always exists unique optimal $\tau_0$ to maximize the identical throughput no matter how many UEs are served in the WPC system. The optimal $\tau_0$ decreases as $K$ increases. In other words, the more UEs are served by the system, the less wireless

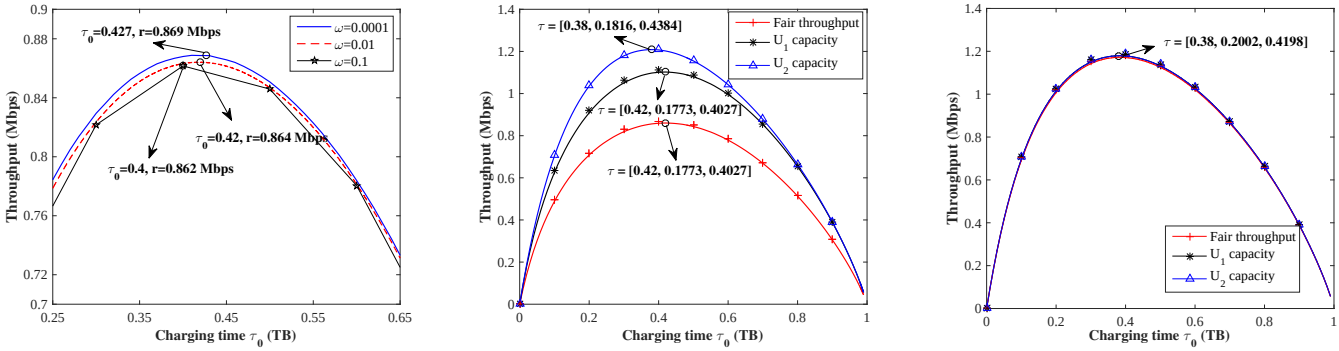


(a) accuracy analysis, $x/L$=20 packets (b) $x/L$=20 packets (c) $x/L$=1000 packets

Fig. 9. Identical buffer-constrained throughput with different time allocation schemes

charging time can be provided to each UE. This is because the system has to allocate more time to the UL transmission to guarantee the max-identical throughput for different UEs which suffer different path losses. Moreover, more users will lead to less transmission time for each UE, which results in the degradation of the identical throughput. In Fig. 11(b), the max-identical throughput are verified as a decreasing function with respect to $K$. However, the overall UL throughput which represents the sum of the throughput of each UE increases in $K$. This phenomenon implies multiplex gain exists in the considered WPC system. Besides, the common throughput in [9] always overestimates the maximum traffic throughput sustained by each UE, since the common throughput is actually equal to the mean channel capacity. It is observed that the gap between the common throughput and max-identical throughput decreases as $K$ increases. However, opposite phenomenon is observed from the point of view of the overall UL throughput. The reason addresses that the multiplex gain for the channel capacity is larger that for the buffer-constrained throughput.

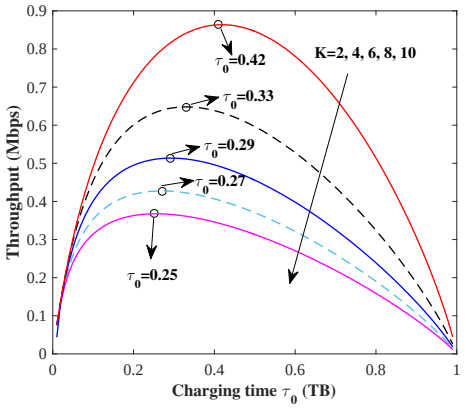


(a) Optimal charging time

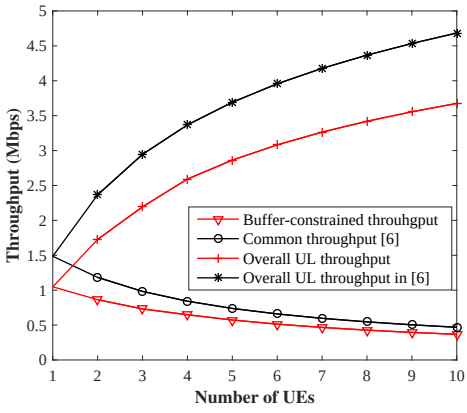


(b) Max-identical throughput

Fig. 11. Max-identical throughput varying with the number of UEs

## VI. Conclusion

In this paper we presented an analytical approach to study buffer-constrained throughput performance of a multi-user wireless powered communication system with consideration of non-linear energy harvesting model, finite energy storage capacity, finite data buffer capacity, stochastic channel and stochastic traffic arrivals. Specifically, the buffer overflow probability is derived based on which the buffer-constrained throughput was then obtained. Furthermore, the minimum DL transmission power and minimum energy storage capacity were studied to ensure the buffer-constraint throughput performance of each node. In the end, an optimal time allocation algorithm was proposed to maximize the minimum throughput which can be guaranteed by each UE simultaneously. We believe, the analysis and the results shed new insights on the performance of WPC systems.

## APPENDIX A
## PROOF OF LEMMA 1

*Proof:* According to (9), we have

$$Pr\{B_k(t) > x_k\} = Pr\{\sup_{0\le s\le t}\{A_k(s,t) - C_k(s,t)\} > x_k\} \tag{24}$$

Let $V_s = e^{\theta_k(A_X(t-s,t)-C_k(t-s,t))}$, $Y_u = A_k(u-1,u)$ and $Z_u = C_k(u-1,u)$. There holds

$$\begin{aligned} V_{s+1} &= e^{\theta_k(A_k(t-s-1,t)-C_k(t-s-1,t))} \\ &= e^{\theta_k\sum_{u=t-s}^{t}(Y_u - Z_u)} \\ &= V_s e^{\theta_k(Y_{t-s}-Z_{t-s})} \end{aligned}.$$

Since $A_k$ and $C_k$ are both i.i.d processes, we have

$$\begin{aligned} &\mathbb{E}[V_{s+1}|V_1, V_2, ...V_s] \\ =&\mathbb{E}[V_{s+1}|Y_t, Y_{t-1}, ...Y_{t-s+1}, Z_t, Z_{t-1}, ...Z_{t-s+1}] \\ =&\mathbb{E}[V_s e^{\theta_k(Y_{t-s}-Z_{t-s})}|Y_t, ...Y_{t-s+1}, Z_t, ...Z_{t-s+1}] \\ \overset{(a)}{=}&\mathbb{E}[V_s|Y_t, ...Y_{t-s+1}, Z_t, ...Z_{t-s+1}]\mathbb{E}[e^{\theta_k Y_{t-s}}]\mathbb{E}[e^{-\theta_k Z_{t-s}}] \\ \overset{(b)}{=}&V_s\mathbb{E}[e^{\theta_k A_k(0,1)}]\mathbb{E}[e^{-\theta_k C_k(0,1)}] \\ \le&V_s \end{aligned}.$$

Here, step (a) is due to $Y_{t-s}$ and $Z_{t-s}$ are independent of each other and also independent of $\{Y_t, Y_{t-1}, ...Y_{t-s+1}, Z_t, Z_{t-1}, ...Z_{t-s+1}\}$. Step (b) holds since processes $A_k$ and $C_k$ are both identical distributed, i.e.,

$$\mathbb{E}[e^{\theta_k Y_{t-s}}] = \mathbb{E}[e^{\theta_k A_k(t-s-1,t-s)}] = \mathbb{E}[e^{\theta_k A_k(0,1)}],$$

$$\mathbb{E}[e^{-\theta_k Z_{t-s}}] = \mathbb{E}[e^{-\theta_k C_k(t-s-1,t-s)}] = \mathbb{E}[e^{-\theta_k C_k(0,1)}].$$

Hence, $V_1, V_2, ..., V_t$ form a non-negative supermartingale [28]. Then, according to the property of the supermartingale. the buffer overflow probability holds as [28, 29]

$$\begin{aligned} &Pr\{B_k(t) > x_k\} \\ =&Pr\{\sup_{0\le s\le t}\{e^{A_k(s,t)-C_k(s,t)}\} > e^{x_k}\} \\ \le&Pr\{\sup_{1\le s\le t}\{V_{t-s}\} > e^{x_k}\} \\ =&Pr\{\sup_{1\le m\le t}\{V_m\} > e^{x_k)}\} \\ \le&Pr\{V_1 > e^{x_k}\} \\ \overset{(a)}{\le}&\mathbb{E}[e^{-\theta_k x_k}]\mathbb{E}[e^{\theta_k A_k(0,1)}]\mathbb{E}[e^{-\theta_k C_k(0,1)}] \\ \le&e^{-\theta_k x_k} \end{aligned}.$$

Step (a) is based on the Chernoff bound and the independence between $A_k$ and $C_k$. Therefore, Lemma 1 is proved. ■

## APPENDIX B
## PROOF OF THEOREM 1

The buffer overflow probability is ascertained by directly applying Lemma 1 and the system stability condition (13). Note that $k = 0$, there holds

$$\begin{aligned} \beta_{\theta_0} &= -\frac{\ln\mathbb{E}[e^{-\theta_0 R_0\tau_0}]}{\theta_0} \\ &= -\frac{\ln\sum_{k=1}^{K}\mathbb{E}[e^{-\theta_0 R_{D_k}\tau_0}]Pr\{k\}}{\theta_0} \end{aligned},$$

which completes the proof.

## APPENDIX C
## PROOF OF THEOREM 2

According to Theorems 1, we have $e^{-\theta_k x_k} = \epsilon_k$, i.e.,

$$\theta_k = -\frac{\ln\epsilon_k}{x_k}.$$

Furthermore, according to the stability condition (16), the maximum traffic envelop rate denoted by $\alpha_{\theta_k}^{\max}$ holds as

$$\alpha_{\theta_k}^{\max} = \beta_{\theta_k}.$$

Besides, the traffic envelop rate $\alpha_{\theta_k}$ is related to the traffic arrival rate $r_k$, which can be denoted by function $g_k(r_k) = \alpha_{\theta_k}$ [23]. Hence, we finally have

$$r_k^{\max} = g_k^{-1}(\alpha_{\theta_k}^{\max}) = g_k^{-1}(\beta_{-\frac{\ln\epsilon_k}{x_k}}),$$

where $g^{-1}(\cdot)$ is the inverse function of $g(\cdot)$.

## APPENDIX D
## PROOF OF THEOREM 3

We first find out $\theta_k$ for each node according to Theorem 1, and there holds

$$\theta_k = -\frac{\ln\epsilon_k}{x_k}. \tag{25}$$

When $1 \le k \le K$, $\beta_{\theta_k}$ is related to DL transmission power $p_0$ through the transmission rate $R_k$ in terms of (6) and (19), i.e.,

$$\beta_{\theta_k} = -\frac{\ln\mathbb{E}[e^{-\theta_k W\log_2(1+\frac{p_k h_k l_k}{N_0 W})\tau_k}]}{\theta_k}, \tag{26}$$

where $p_k = \pi_k\frac{1-e^{-\nu_1(p_0 h_k l_k - p_D)}}{1+e^{-\nu_1(p_0 h_k l_k - p_D-\nu_2)}}\frac{\tau_0}{\tau_k}$ according to (2), (4) and (5).

When $k = 0$, jointly considering (3) and (19), we have

$$\beta_{\theta_0} = -\frac{\sum_{k=1}^{K}\mathbb{E}[e^{-\theta_0 W\log_2(1+\frac{p_0 h_k l_k}{N_0 W})\tau_0}]Pr\{k\}}{\theta_k}. \tag{27}$$

In addition, by applying the stability condition (16), there holds

$$\beta_{\theta_k} \ge \alpha_{\theta_k} = g_k(r_k).$$

As $\beta_{\theta_k}$ increases with $p_0$ for any $0 \le k \le K$, the minimum DL transmission power required by each nodes, denoted by $p_{0,k}$, is the solution of following equation

$$\beta_{\theta_k} = g_k(r_k). \tag{28}$$

Therefore, $p_{0,k}(0 \le k \le K)$ is ascertained for each node by solving the equation set consisting of (25), (26), (27) and (28). Thereafter, we should choose the maximum $p_{0,k}$ as the

transmission power such that the performance requirement of each node can be guaranteed. There holds,

$$p_0^{\min} = \max\{p_{0,k} : 0 \leq k \leq K\}.$$

Thus, the proof is completed.

## REFERENCES


[1] Y. Zeng, B. Clerckx, and R. Zhang, "Communications and signals design for wireless power transmission," *IEEE Trans. on Commun.*, vol. 65, no. 5, pp. 2264–2290, May 2017.

[2] X. Lu, P. Wang, D. Niyato, D. I. Kim, and Z. Han, "Wireless charging technologies: Fundamentals, standards, and network applications," *IEEE Commun. Sur. Tuts.*, vol. 18, no. 2, pp. 1413–1452, Secondquarter 2016.

[3] S. Bi, C. K. Ho, and R. Zhang, "Wireless powered communication: Opportunities and challenges," *IEEE Commun. Mag.*, vol. 53, no. 4, pp. 117–125, April 2015.

[4] S. Bi, Y. Zeng, and R. Zhang, "Wireless powered communication networks: an overview," *IEEE Wireless Commun.*, vol. 23, no. 2, pp. 10–18, April 2016.

[5] D. Niyato, D. I. Kim, M. Maso, and Z. Han, "Wireless powered communication networks: Research directions and technological approaches," *IEEE Wireless Commun.*, vol. 24, no. 6, pp. 88–97, Dec 2017.

[6] S. Ulukus, A. Yener, and et al., "Energy harvesting wireless communications: A review of recent advances," *IEEE J. Sel. Areas Commun.*, vol. 33, no. 3, pp. 360–381, March 2015.

[7] E. Boshkovska, D. W. K. Ng, N. Zlatanov, A. Koelpin, and R. Schober, "Robust resource allocation for mimo wireless powered communication networks based on a non-linear eh model," *IEEE Trans. Commun.*, vol. 65, no. 5, pp. 1984–1999, May 2017.

[8] G. Pan, H. Lei, Y. Yuan, and Z. Ding, "Performance analysis and optimization for SWIPT wireless sensor networks," *IEEE Trans. Commun.*, vol. 65, no. 5, pp. 2291–2302, May 2017.

[9] H. Ju and R. Zhang, "Throughput maximization in wireless powered communication networks," *IEEE Trans. Wireless Commun.*, vol. 13, no. 1, pp. 418–428, January 2014.

[10] Y. L. Che, L. Duan, and R. Zhang, "Spatial throughput maximization of wireless powered communication networks," *IEEE J. Sel. Areas Commun.*, vol. 33, no. 8, pp. 1534–1548, Aug 2015.

[11] D. Hwang, D. I. Kim, and T. J. Lee, "Throughput maximization for multiuser MIMO wireless powered communication networks," *IEEE Trans. Veh. Technol.*, vol. 65, no. 7, pp. 5743–5748, July 2016.

[12] W. Huang, H. Chen, Y. Li, and B. Vucetic, "On the performance of multi-antenna wireless-powered communications with energy beamforming," *IEEE Trans. Veh. Technol.*, vol. 65, no. 3, pp. 1801–1808, March 2016.

[13] R. Morsi, E. Boshkovska, E. Ramadan, D. W. K. Ng, and R. Schober, "On the performance of wireless powered communication with non-linear energy harvesting," in *2017 IEEE 18th International Workshop on Signal Processing Advances in Wireless Communications (SPAWC)*, July 2017, pp. 1–5.

[14] X. Zhou, R. Zhang, and C. K. Ho, "Wireless information and power transfer: Architecture design and rate-energy tradeoff," *IEEE Trans Commun.*, vol. 61, no. 11, pp. 4754–4767, November 2013.

[15] R. Zhang and C. K. Ho, "Mimo broadcasting for simultaneous wireless information and power transfer," *IEEE Trans. Wireless Commun.*, vol. 12, no. 5, pp. 1989–2001, May 2013.

[16] K. Xiong, B. Wang, and K. J. R. Liu, "Rate-energy region of SWIPT for MIMO broadcasting under nonlinear energy harvesting model," *IEEE Trans. Wireless Commun.*, vol. 16, no. 8, pp. 5147–5161, Aug 2017.

[17] I. M. Kim, D. I. Kim, and J. M. Kang, "Rate-energy tradeoff and decoding error probability-energy tradeoff for SWIPT in finite code length," *IEEE Trans. Wireless Commun.*, vol. 16, no. 12, pp. 8220–8234, Dec 2017.

[18] J. Yang, Q. Yang, and et al., "Power-delay tradeoff in wireless powered communication networks," *IEEE Trans. Veh. Technol.*, vol. 66, no. 4, pp. 3280–3292, April 2017.

[19] Q. Yao, A. Huang, and et al., "Delay-aware wireless powered communication networks: Energy balancing and optimization," *IEEE Trans. Wireless Commun.*, vol. 15, no. 8, pp. 5272–5286, Aug 2016.

[20] Z. Li, Y. Jiang, Y. Gao, P. Li, L. Sang, and D. Yang, "Delay and delay-constrained throughput performance of a wireless-powered communication system," *IEEE Access*, vol. 5, pp. 21 620–21 631, 2017.

[21] X. Wang, T. Yu, and Y. Xu, "Lower bound for node buffer size in intermittently connected wireless networks," *IEEE Trans. Parallel Distrib. Syst.*, vol. 24, no. 4, pp. 754–766, April 2013.

[22] X. Chen, C. Yuen, and Z. Zhang, "Wireless energy and information transfer tradeoff for limited-feedback multiantenna systems with energy beamforming," *IEEE Trans. Veh. Technol.*, vol. 63, no. 1, pp. 407–412, Jan 2014.

[23] Y. Jiang and Y. Liu, *Stochastic Network Calculus*. London, U.K.: Springer, 2008.

[24] C. Li, A. Burchard, and J. Liebeherr, "A network calculus with effective bandwidth," *IEEE/ACM Trans. on Netw.*, vol. 15, no. 6, 2007.

[25] Y. Jiang, "A note on applying stochastic network calculus. http://q2s.ntnu.no/ jiang/publications.html," 2010.

[26] F. Sun and Y. Jiang, "A statistical property of wireless channel capacity: Theory and application," *Performance Evaluation Review*, vol. 45, no. 4, pp. 97–108, December 2017.

[27] M. K. Simon and M.-S. Alouini, *Digital communication over fading channels*. New York, NY, USA: Wiley, 2005.

[28] J. L. Doob, *Stochastic processes*. New York, NY, USA: Wiley, 1953.

[29] J. F. C. Kingman, "A martingale inequality in the theory of queues," *Mathematical Proceedings of the Cambridge Philosophical Society*, vol. 60, no. 60, pp. 359–361, 1964.